Mesoscale forecasts of stratospheric mountain waves

Andreas Dörnbrack, Martin Leutbecher, Hans Volkert and Martin Wirth,
DLR-Oberpfaffenhofen, Institut für Physik der Atmosphäre, D-82230 Weßling, Germany

A forecasting system was set up to infer the impact of mountain waves for producing mesoscale temperature anomalies in the stratosphere. It was successfully applied during a recent aircraft campaign which operated out of Rovaniemi, northern Finland, between 18 December 1996 and 15 January 1997. The forecast information led to the successful detection of mountain-induced polar stratospheric clouds on 9 January 1997. For this event mesoscale forecasts, hindcast runs including grid nesting and comparisons with lidar observations and radiosonde measurements are presented.

1. Introduction

The discovery of the 'ozone hole' above Antarctica at the end of the polar night sparked off strong interest not only in stratospheric chemistry, but also in atmospheric dynamics in the height interval between 20 and 30 km. Polar stratospheric clouds (PSC), more precisely regions of enhanced aerosol concentration of, for example, nitric acid trihydrate or ice particles, are of particular interest for investigations regarding the ozone budget in this height range. Of prime importance are the questions *whether*, to *what extent* and for *how long* the air temperature falls below the threshold value for PSC formation.

In recent years a number of international campaigns have been launched to probe PSC remotely using, for example, upward looking ground based or airborne lidars, or *in situ* measurements (e.g. with balloon-borne instruments). During the northern hemisphere missions EASOE (European Arctic Stratospheric Ozone Experiment; 1991/92) and SESAME (Second European Stratospheric Arctic and Mid-latitude Experiment; 1994/95) techniques were refined to determine air parcel trajectories from global forecasts for mission guidance and from global analyses for data interpretation (cf. Pyle *et al.*, 1993, for an overview and Lefevre *et al.*, 1994 for a large-scale application). Mesoscale temperature anomalies, which are induced by upward propagating gravity waves in strong cross-mountain flow and which extend some hundreds of kilometres horizontally, were identified as providing an explanation of some of the not too infrequent discrepancies of several degrees between observed and global-scale temperatures (e.g. Volkert & Intes, 1992). Operational mesoscale numerical weather prediction (NWP) models could not directly be used to infer realistically these stratospheric anomalies, because they possess only very few stratospheric levels.

Therefore, a research-type NWP model (MM5) was specifically applied to the situation above Scandinavia and its extended mountain ranges: this includes a suitable horizontal grid length (36 or 12 km), a sufficiently large domain (2200 by 2200 km²) and a good vertical resolution (52 levels between the ground and 29 km). This model set-up driven by archived analyses was first used for the mountain wave event of 23 January 1991 (Leutbecher & Volkert, 1996).

Demands from the steering groups of the combined German and European aircraft campaigns POLECAT (polar stratospheric clouds, lee waves, chemistry, aerosols and transport; see Peter *et al.*, 1995 for an overview) and APE (Airborne Polar Experiment) regarding detailed mission guidance resulted in the *ad hoc* installation of a forecasting system. This consisted of MM5 mesoscale forecasts driven by the routine global forecast data of Deutscher Wetterdienst (DWD).

The purpose of this documentation is to introduce briefly the forecast system (section 2), to exemplify the forecast for one particular mission day (section 3) and to compare the forecast and subsequent hindcasts with independent measurements (section 4). A discussion of the forecasts, hindcasts and their quality control concludes the paper, whereas a detailed interpretation of the mission results will be given elsewhere.
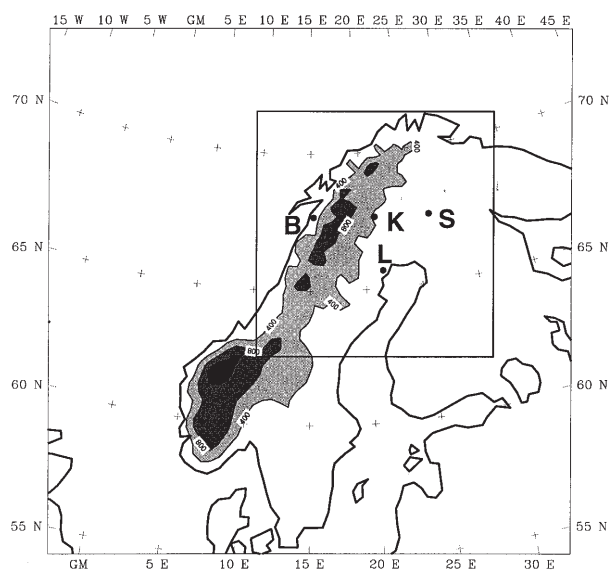
2. Forecast system

The fifth generation Pennsylvania State University/National Center for Atmospheric Research mesoscale model (MM5; see Dudhia, 1993 and Grell *et al.*, 1994) is used as the core component to forecast mesoscale temperature anomalies in the stratosphere above Scandinavia. The model is driven by forecast data from the Global-Modell (GM) of DWD. Both components are introduced in the following.

2.1. Mesoscale model MM5

The MM5 model integrates the fully compressible set of equations in a rotating frame of reference. In the non-hydrostatic version used here, the prognostic variables are velocity (u, v, w), pressure perturbation p', and temperature T.

In forecast mode a 'coarse' horizontal resolution of 36 km was used (61×61 meshes; 2200 km domain length). After the mission two simulations are performed: a control run with the coarse forecast resolution and one using a two-way interactive grid-nesting scheme. This 'fine' resolution run contains a nest with a grid size of 12 km (82×82 meshes; 984 km subdomain length; see Figure 1) to resolve better the orography and the resultant wave development. The vertical resolution was about 0.58 km in both modes with a total of 52 levels. The model top is at 10 hPa (≈ 29 km). At the upper boundary a radiative boundary condition avoids the reflection of vertically propagating gravity waves. Terrain heights on the coarse (fine) grid were obtained by interpolation from a 5' (30") orographic data set provided by the Geophysical Data Center (Boulder, USA).

As the major source for gravity waves in the stratosphere are mountain waves, moist processes were considered unimportant and were therefore switched off. The time scale for radiative cooling in the stratosphere is longer than the time scale for advection through the mesoscale domain; thus, it seemed legitimate to neglect radiative processes. The momentum flux at the lower boundary is parameterised via a bulk aerodynamic drag term with a coefficient that depends on the mountain height (equivalent to a roughness length of up to a few decimetres). Turbulent mixing in the free atmosphere is taken into account by vertical diffusion, which depends on the local Richardson number.
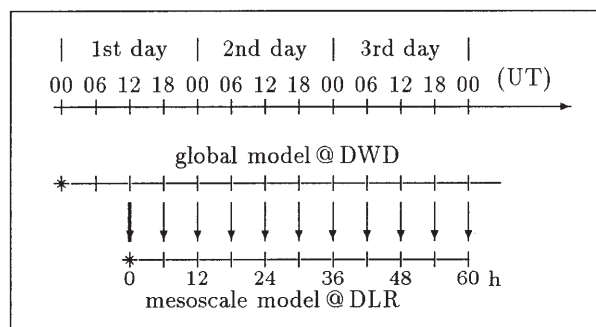
2.2. Initial and boundary data

The boundary and initial conditions for the MM5 model were supplied from global forecasts and, after the event, also from analyses by the Central Office of DWD in Offenbach, Germany. These data were obtained daily with a spatial resolution of 1.5° in latitude and longitude and on 15 standard pressure levels from the surface to 10 hPa.

The GM has been in operational use since early 1991. It constitutes an offspring of the ECMWF spectral model. It is operated at a resolution of 106 horizontal wave numbers (T106; equivalent to a grid length of about 125 km) and with 19 layers in the vertical (Schrodin, 1996).

Each morning 13 GM-datasets were received, spanning the 72 h period starting the previous midnight in 6 h intervals. The mesoscale model was initialised for 1200 UT and its forecast carried over 60 h (see Figure 2). At about noon the mesoscale forecast information was available and a set of maps and cross-sections was forwarded to the operation centre in Rovaniemi.

3. Forecast of a wave event

During the second half of December 1996 the temperature fields from the GM and MM5 forecasts differed only marginally as the atmospheric conditions were not conducive to a combination of wave excitation at low levels and wave propagation to stratospheric levels. At the beginning of January 1997 the situation gradually changed. On 7 January a distinct wave event first appeared in the forecasts for 9 January. In this section we concentrate on this event by first sketching the background weather situation as it was observed on 9 January and by then presenting the forecast material.

Figure 1. *Computational domain of the mesoscale model covering Scandinavia and the Norwegian Sea. The model orography is given in increments of 400 m. Locations: Bodø (B), Kiruna (K), Luleå (L), Sodankylä (S). The box shows the nested region used in the hindcasts.*

Figure 2. *Schedule of the daily forecast cycle. The global model is initialised (*) at 0000 UT; the mesoscale model is initialised with the 1200 UT forecast of the global model. Boundary conditions are updated from the global forecast data every six hours.*
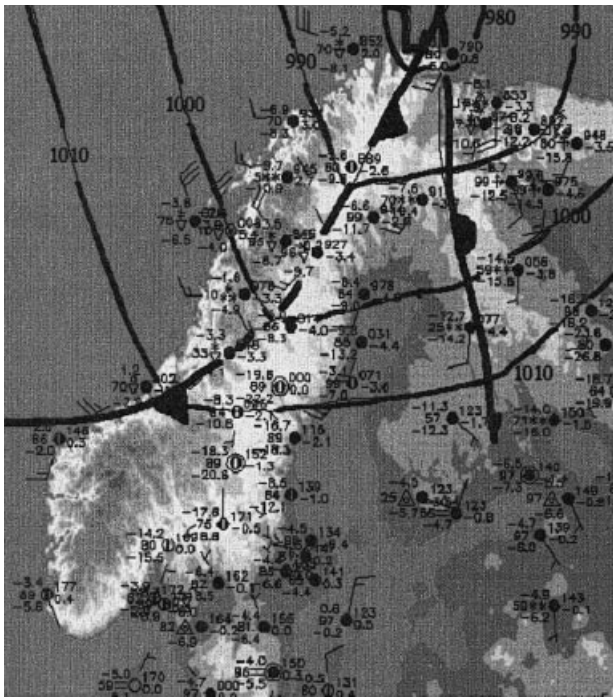
Figure 3. *Surface weather chart for 1200 UT on 9 January 1997 with station reports and manual pressure analysis (increment: 10 hPa; adapted from the regular World Wide Web information provided by Universität Karlsruhe, Germany).*
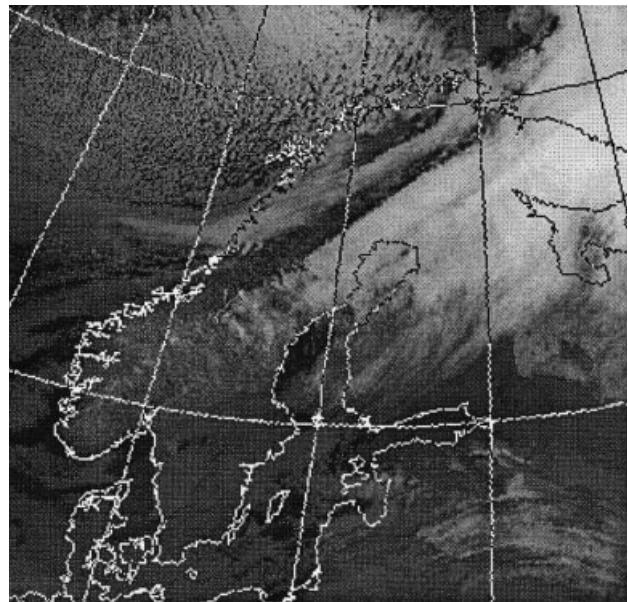

Figure 4. *Infrared NOAA-14 satellite image (channel 4) for 1142 UT on 9 January 1997 (adapted from the regular World Wide Web information provided by University of Dundee, UK).*

3.1. Background weather situation

At midday on 9 January a fast moving cold front at the leading edge of a strong cold air outbreak from the Arctic had reached and partly crossed the Scandinavian mountains (Figure 3). It belonged to an intense surface depression (970 hPa core pressure) east of North Cape which had moved from Spitsbergen during the previous 24 h and had intensified by about 20 hPa. The 12 hourly soundings from Bodø on the Norwegian coast (symbols in Figure 5) indicate at lower levels an initial shift in wind direction from north-easterly to south-westerly followed by a change to north-westerlies after the passage of the front together with a distinct increase in speed (up to 25 m s^{-1} below 800 hPa at 1200 UT).

Another kind of synopsis is given by an infrared satellite image at noon (Figure 4). Three distinct cloud features are present over Northern Scandinavia and the Norwegian Sea:

(a) shower clouds within the cold-air outbreak over the sea;
(b) an elongated, optically thick cloud band in the position of the surface cold front; and
(c) an extensive cirrus shield overlaying the warm sector of the surface depression.

Most remarkable, however, is the distinct gap, some 1000 km in length, between the cirrus shield and the frontal cloud. This is indicative of subsidence in the tropopause level, which could be induced by mountain

waves. The gap also showed up in the satellite images of 0715 UT, and was much wider in that of 1705 UT. It was a persistent feature of that day.

The Bodø sounding at 1200 UT (Figure 5; sounding (*c*)) reveals the prerequisites for the excitation and possible propagation of mountain waves to stratospheric levels: a strong wind at mountain crest height (about 20 m s^{-1}) as well as a flow perpendicular to the ridge and little directional shear with height (270 ± 15°).

The question remains as to what extent this situation was forecast on the previous day for mission planning purposes.

3.2. Forecast and mission

For detailed mission planning it was necessary, first, to infer the stratospheric background temperatures as forecast by the global model and, secondly, to check whether the flow configuration is conducive to producing distinct mesoscale temperature anomalies. Therefore, GM and MM5 results were juxtaposed. The temporal evolution of the temperature field on the 560 K isentropic surface (i.e. at a height of about 23 km) during 9 January is given in Figure 6. The GM predicted a quasi-stationary field with a uniform north–south gradient (e.g. 11 K/1000 km along 20° E). Only a slight undulation of the isotherms above the Lofoden Islands at 1800 UT points to a possibly orographically caused deformation. In the MM5 forecast, however, a distinct mesoscale temperature contrast developed from $\Delta T \approx 2$ K at 0600 UT via $\Delta T \approx 4$ K at 1200 UT to $\Delta T \approx 9$ K at 1800 UT over a distance of 200 km in an area above and downstream of the
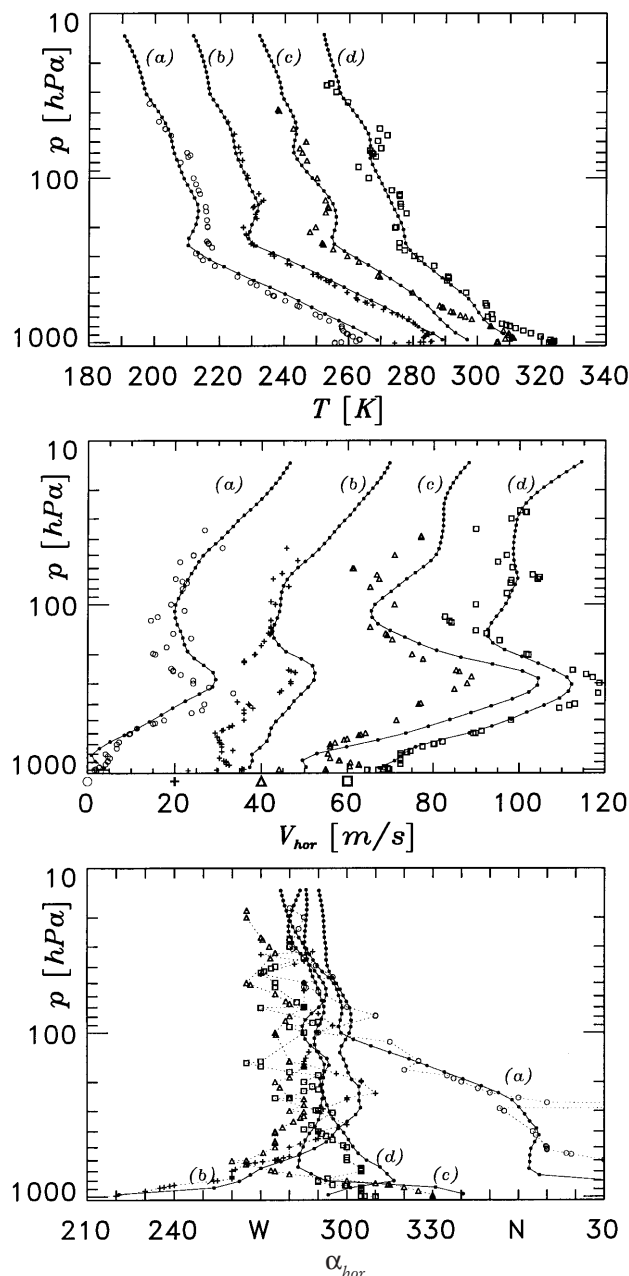
Figure 5. *Radiosondes and model profiles of temperature (top), horizontal wind speed (middle) and wind direction (bottom) for Bodø, (see Figure 1) at 1200 UT on 8 January (a, o), at 0000 UT (b, +) and 1200 UT on 9 January (c, Δ) and at 0000 UT on 10 January 1997 (d, □). The measurements are marked by symbols and the model profiles by solid lines with dots indicating the model levels. Temperature profiles (b) to (d) are shifted by 20 K each and the corresponding velocity profiles by 20 m s⁻¹. The origin of each velocity profile is marked by its enlarged symbol beneath the abscissa.*

northern Scandinavian mountains. The anomaly pattern was forecast to move gradually southwards during the afternoon while a second cold spot developed further downstream. At 1800 UT a warm–cold–warm pattern with a horizontal wavelength of about 400 km and a north–south extent of some 500 km was established and predicted to stay for at least 6 h.

A cross-section through the temperature minimum at

1800 UT (191.5 K) and parallel to the wind field in 30 hPa indicates two cold tongues aligned with an upward displacement of the potential temperature surfaces (Figure 7). At this time the minimum forecast temperatures were suggesting that the threshold value for PSC formation might be reached. Similar indications had already appeared in the 54 h forecast initialised at noon on 7 January.

Therefore, a flight mission was scheduled for and eventually undertaken on 9 January between 1500 and 1930 UT with several flight legs along and parallel to the section in Figure 7. The upward looking lidar on board the Falcon research aircraft (see Wirth & Renger, 1996 for technical specifications) encountered three isolated PSC, two above Kiruna separated in time by some 3 hours and one further to the east above Sodankylä. The Lidar image of the first encounter (Figure 8) reveals a highly reflective structure of about 160 km horizontal extent in the height range of 24 to 27 km. Within the horizontal accuracy of, say, two grid lengths (70 km) the western edge of the structure coincides with the predicted temperature minimum. The succession of some ten waves, gradually fading from west to east along the flow direction, is too fine a feature to be resolved by the MM5 forecast.

The second encounter above Sodankylä is colocated with the other temperature minimum downstream, while the third PSC was again found within the first 'cold spot'. So, the mesoscale model guidance had obviously enabled the experimenters to detect features they were interested in finding, amidst the darkness of the polar night.

4. Comparison with observations

A hindcast with the 'coarse' spatial resolution as in the forecast mode (36 km) but driven with the GM analyses for the 36 h period from 8 January 1200 UT as 'true' initial and boundary values served as a first quality control step regarding the forecast data. It yielded a very similar stratospheric temperature pattern (Figure 9, as compared with Figure 6 bottom) but consistently warmer by 1 to 2 K as the global analyses were warmer, too.

In a second hindcast integration a nested region with threefold horizontal resolution (12 km) was defined completely covering the mesoscale temperature anomalies (cf. Figure 1 and Figure 10). From previous experience it was expected that a better resolved orography would lead to a larger wave response and lower temperature minima. For the following more detailed comparisons all model data stem from this fine mesh hindcast.
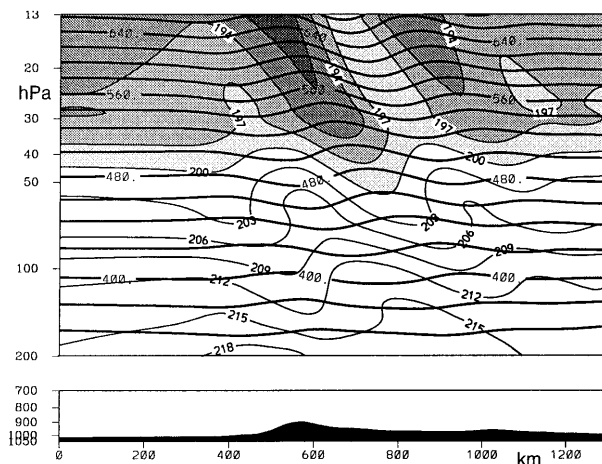
4.1. Model versus Lidar

As in the coarse mesh hindcast, two cold spots develop
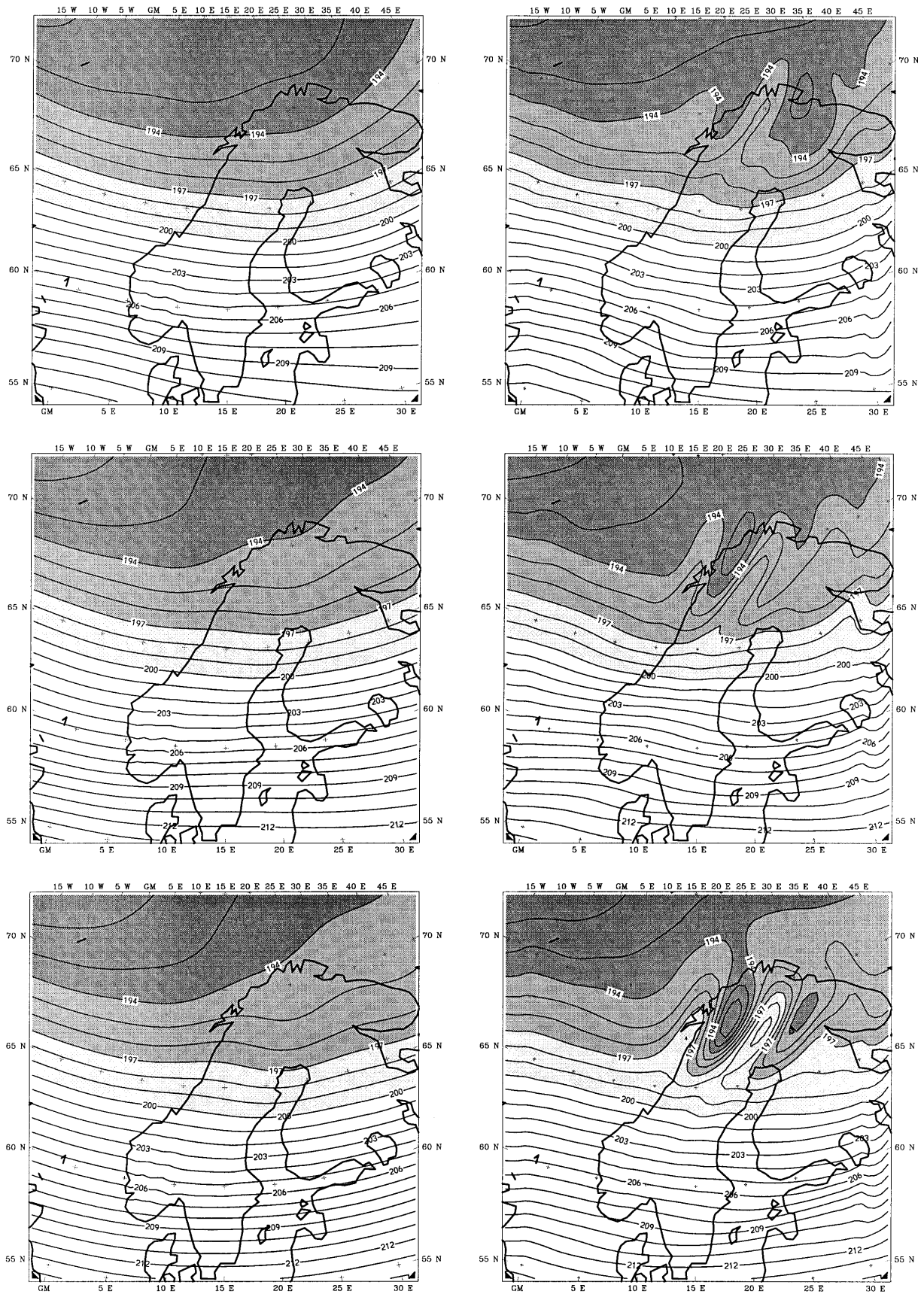
Figure 6. *Forecasts of temperature on the 560 K potential temperature surface for 0600 (+18 h), 1200 (+24 h) and 1800 UT (+30 h) on 9 January 1997 (from top to bottom); GM (left) and MM5 results (right); values in K.*

Figure 7. *Vertical section through the 1800 UT forecast given in Figure 6; temperature (thin lines; increment: 3 K) and potential temperature (thick lines; increment: 20 K) in the stratosphere. The terrain height is indicated at the bottom.*

on the 560 K potential temperature surface: one above the main ridge and the other some 300 to 400 km downstream to the north of the Gulf of Bothnia (Figure 10). But the structures in the fine mesh hindcast are more confined (maximum gradient: 9 K/70 km at 1800 UT) and the minimum temperatures up to 7 K lower than in the coarse mesh run. The lowest values around 186 K are within 1 K of the threshold temperature below which ice particles form at 30 hPa with an assumed water vapour concentration of 5 ppmv (Hanson & Mauersberger, 1988).

Two vertical sections through the 1800 UT chart are of special interest (Figure 11). The one through the regular sounding stations at Bodø and Sodankylä indicates how both cold spots coincide with upward displacements of the isentropic surfaces by up to 1.8 km (equiv-

alent to $\Delta T = 18$ K) along the 600 K isentrope above Sodankylä. The other, aligned with the lidar measurement (cf. Figure 8), underpins the hypothesis that the observed mountain-induced PSC begins abruptly within the temperature minimum and gradually fades away across the downstream side of the cold spot. Any fine-scale structures as the succession of some ten waves are significantly beyond the resolution of even the nested domain.

4.2. Model versus radiosonde soundings

The vertical variation of meteorological parameters is operationally measured at radiosonde stations every 12 h (0000 and 1200 UT) and at some stations also at the intermediate times (0600 and 1800 UT). Bodø (Norway) provided 12 hourly upstream profiles for our area of interest, and Luleå (Sweden) and Sodankylä (Finland) could be used as downstream soundings (some 300 km off the main mountain ridge).

The standard and significant level data (typically less than 50 levels per sounding) as distributed over the international meteorological network are compared with the 52 model levels in a vertical column that is closest to the station location (Figure 5 for Bodø and Figure 12 for Luleå) for all available soundings during the hindcast period. The general features in the measurements of the tropospheric and stratospheric temperature structures, the temporal variation of the tropopause height and the evolution of a jet maximum below the tropopause are well captured by the model analysis (i.e. global analysis interpolated to the MM5 grid) and the nested hindcast. But discrepancies are also apparent, especially at stratospheric levels where the model data exhibit a smaller variability with height than the observations.
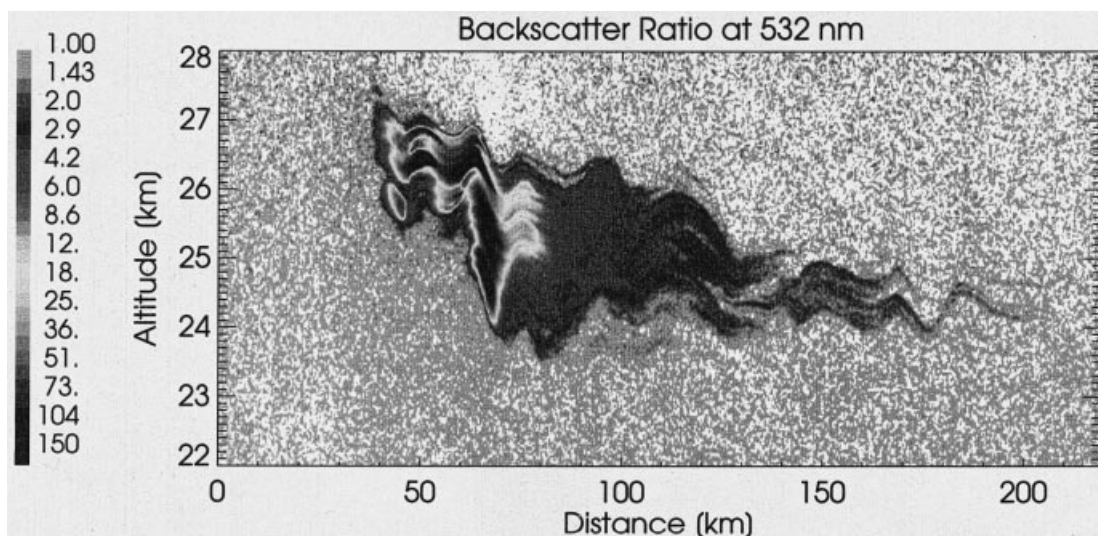
Figure 8. *LIDAR back-scattering ratio as observed near Kiruna (left edge at 68.2° N, 17.9° E; right edge at 67.3° N, 22.4° E) between 1600 and 1625 UT on 9 January 1997.*
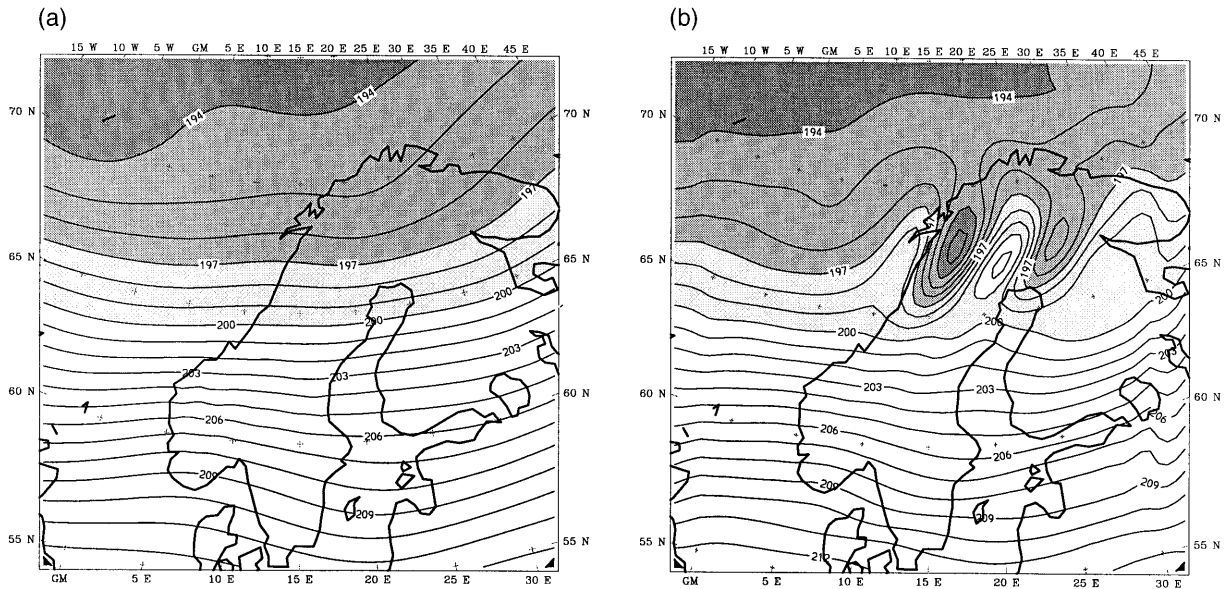
Figure 9. *Temperature on the 560 K potential temperature surface for 1800 UT on 9 January 1997 for (a) GM (analysis) and (b) MM5 result (+ 30 h hindcast); values in K.*
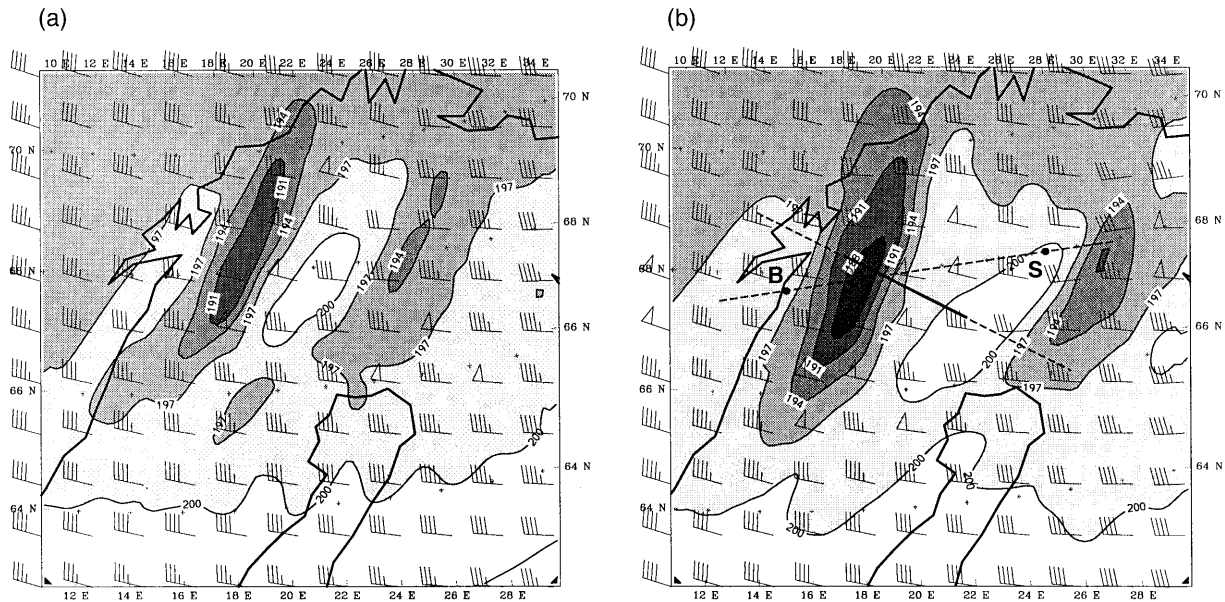

Figure 10. *Hindcasts of temperature on the 560 K potential temperature surface in the nested domain at (a) 1200 UT (+ 24 h) and (b) 1800 UT (+ 30 h) on 9 January 1997; values in K; straight lines indicate the sections shown in Figure 11.*

Shutts *et al.* (1988) have already pointed out that stratospheric gravity waves can be seen in complete sounding data, which at present provide a data point every 2 or 10 seconds. In our case such data are only available from Sodankylä (up to 2700 data points, or 60 times as many as are distributed over the conventional WMO channels; Figure 13). The model analysed temperature and wind profiles (curves (*a*)) represent a remarkable accordance with the observations, very much as though they were obtained as a running mean through the many measured smaller variations. During the hindcast period (curves (*b*) to (*d*)) the gravity wave activity is noticed in the observations and in the model.

However, there is a systematic phase shift between both kinds of data, especially at stratospheric levels. Still, the gradual lowering of the tropopause (which cannot be recognised clearly above the other stations) is well covered as is the speed-up over 24 h of the tropospheric jet from 28 to 41 m s⁻¹ (curves (*b*) and (*d*)).

The horizontal temperature structure on the 560 K surface (about 30 hPa) cannot be verified with observations in any detail as all stations are at some distance from the cold spot and as most balloons did not reach sufficiently high. At 1800 UT above Sodankylä there is a good correspondence at 20 hPa (191 K in Figure 11;

123
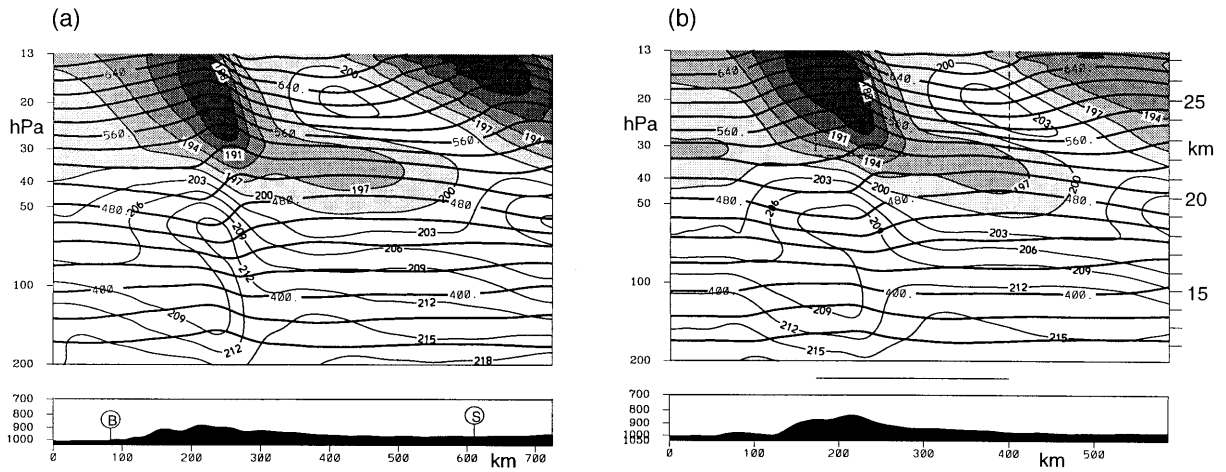
Figure 11. *Vertical sections of temperature (thin lines every 3 K) and potential temperature (thick lines every 20 K) in the nested domain at 1800 UT on 9 January 1997 (+ 30 h hindcast): (a) through Bodø (B) and Sodankylä (S) emphasising the stratospheric temperature contrast and (b) along the flight path of Falcon (marked by a bar above topography; the area corresponding to Figure 8 has a dashed circumference).*
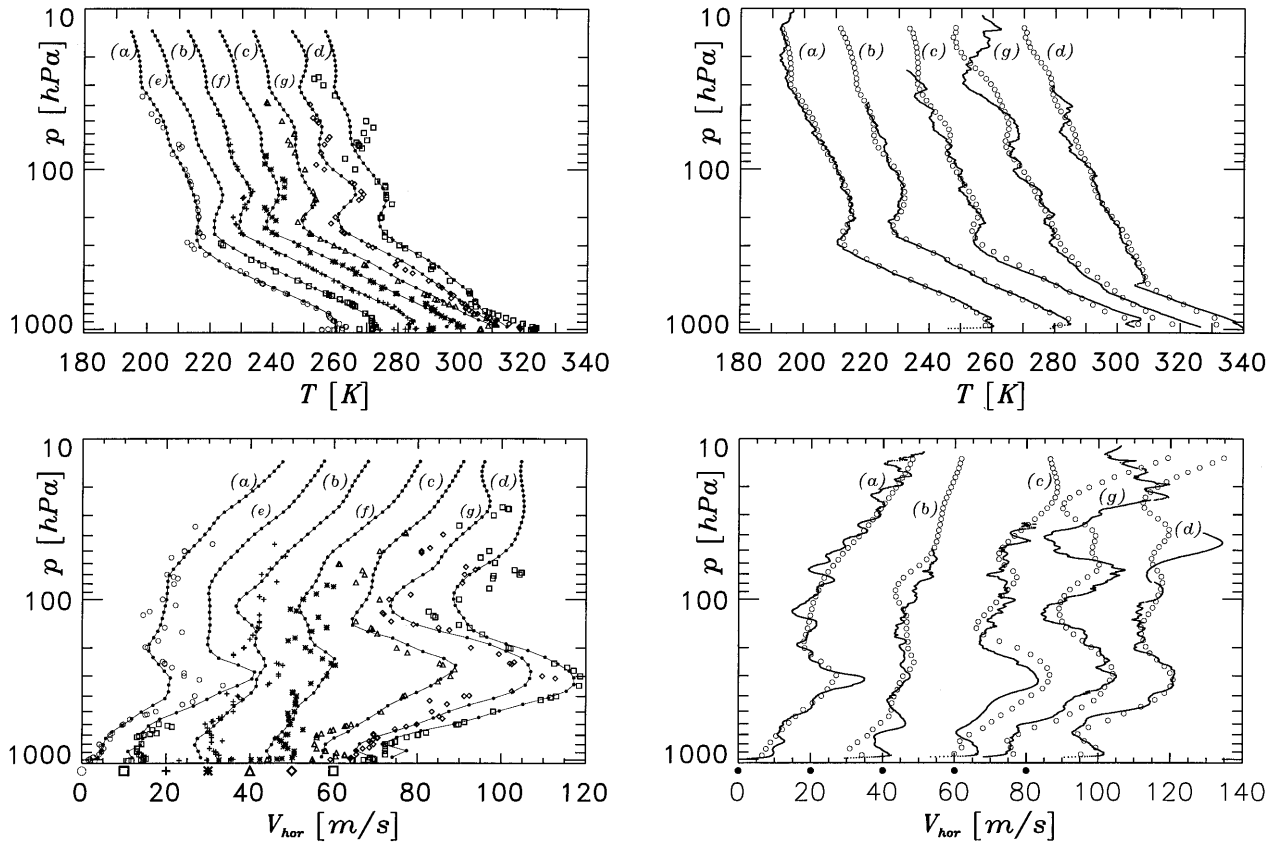
Figure 12. *Radiosonde and model profiles of temperature (top) and horizontal wind speed (bottom) for Luleå (see Figure 1) at the main observation times as in Figure 5, i.e. at 1200 UT on 8 January (a, o), at 0000 UT (b, +) and 1200 UT on 9 January (c, Δ) and at 0000 UT on 10 January 1997 (d, □), and at the intermediate 1800, 0600, 1800 UT ascents (e to g). The measurements are marked by symbols and the model profiles by solid lines with dots indicating the model levels. Subsequent temperature profiles are shifted by 10 K each and the corresponding velocity profiles by 10 m s⁻¹. The origin of each velocity profile is marked by its enlarged symbol beneath the abscissa.*

Figure 13. *Fine resolution radiosonde and model profiles of temperature (top) and horizontal wind speed (bottom) for Sodankylä (see Figure 1). The radiosonde data are plotted with continuous dots (every 2 s ≈ 10 m); the model profiles are marked by open circles. (a) to (d) and (g) refer to the same times as in Figure 12, each being shifted by 20 K or 20 m s⁻¹ from the preceding one.*
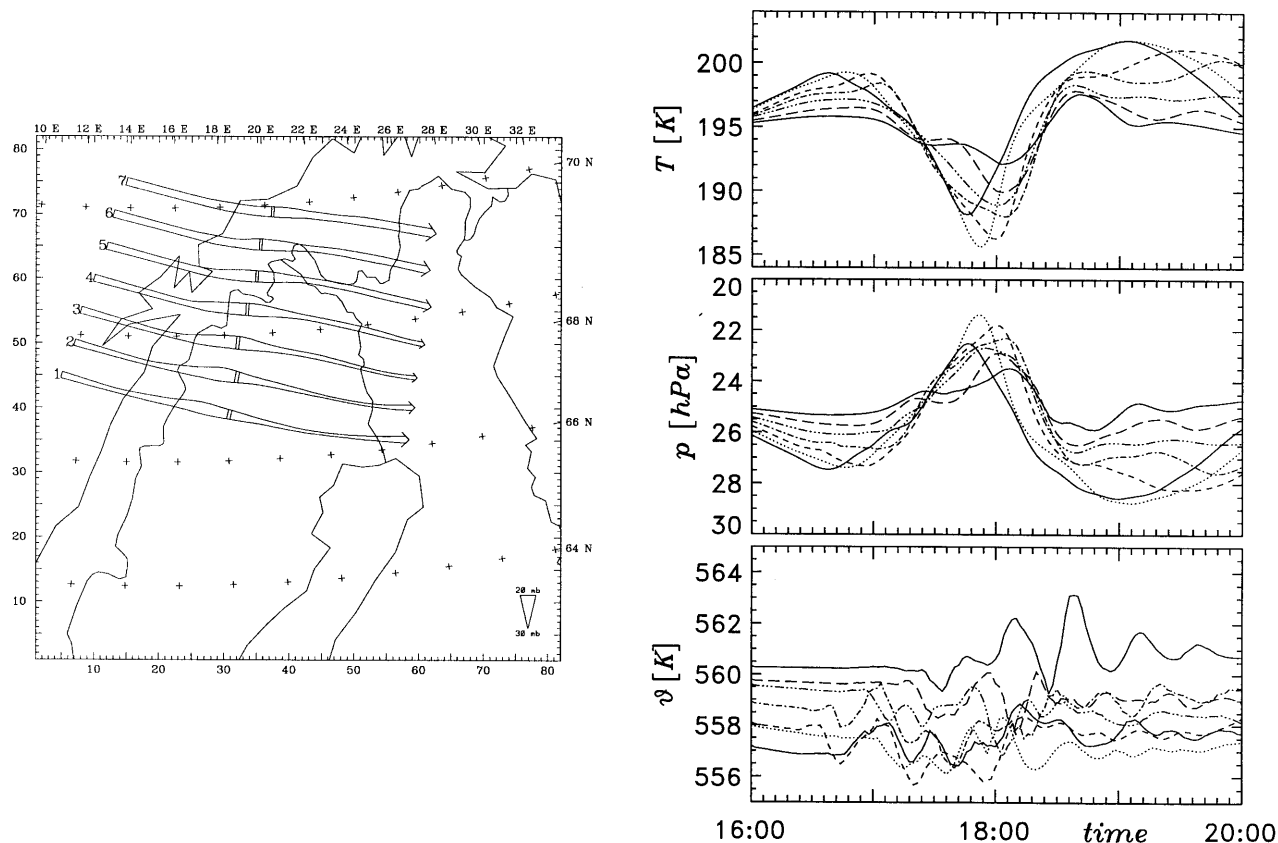
Figure 14. *Left panel: Trajectories of massless particles started in the nested domain at 1600 UT on 9 January 1997 at about 23 km. The thickness of the line corresponds to the actual pressure level. The trajectories terminate at 2000 UT. Right panels from top to bottom: Histories of temperature, pressure and potential temperature along the individual trajectories. Line coding from south to north is as follows. No 1:———; No 2:·······; No 3:----; No 4:-·-·-; No 5:-··-··; No 6:———; No 7:———.*

193 K observed), but a large discrepancy at 30 hPa (201 K in Figure 11; 191 K observed). We note that the horizontal drift of the balloon should be taken into account for detailed comparisons (with a mean unidirectional wind of 35 m s^{-1} the balloon is blown some 170 km during the 80 min till it reaches the 20 hPa level!).

5. Conclusion and outlook

We have demonstrated how a specialised forecasting tool for the support of stratospheric field campaigns can be set up by feeding a three-dimensional mesoscale model (MM5) with actual large-scale forecast data (GM of DWD). The technical prerequisites are fairly standard, i.e. an electronic link to the regular forecasting centre (Offenbach in our case) for near-real-time data transfer and a high-speed computer system (Cray J916 in our case) to carry through the 60 h mesoscale forecast within a few 'wall-clock' hours.

The discussed mission of 9 January was especially successful as the quite transient mesoscale PSC above the mountains and in the lee could only be detected through the guidance of the mesoscale forecast. During the campaign (16 December 1996 till 15 January 1997) a few other occasions with mountain-induced temper-

ature anomalies occurred (e.g. on 7, 12, 15 January) but they had not been probed as either the temperature level was too high for PSC formation or other conflicting mission objectives got priority or the wave region was over southern Norway and, thus, too far from Rovaniemi. Two further successful missions (28 January and 1 February 1997) guided by MM5 forecasts were carried out during the follow-on POLSTAR (Polar Stratospheric Aerosol Experiment) campaign which was based in Kiruna and concentrated *inter alia* on the tropopause region above the Scandinavian mountains. A common experience was that the 'coarse' mesh forecasts provided reliable guidance for the location and time of appearance of cold spots, while the strength of the anomalies was systematically underestimated. 'Fine' mesh integrations, which are presently only possible in hindcast mode, tend to reduce this underestimation significantly.

It appears that mesoscale simulations with high horizontal and vertical resolution are also indispensable for a thorough interpretation of the various measurements. For instance, microphysical studies can use trajectory calculations using the MM5 output fields (Figure 14) to investigate the impact of a cooling by 13 K over one hour (trajectory no. 2) followed by a warming of the same amount in only half the time.

A Dörnbrack, M Leutbecher, H Volkert and M Wirth

Furthermore, we note that the presented temperature anomalies (Figure 10) are not really covered by routine radiosonde soundings. For future campaigns additional high-reaching temperature and wind profiles are to be organised. Additionally, the high-resolution raw data of the existing soundings (as in Figure 13) should be made accessible to the research community. In our case the Bodø sounding at 0000 UT on 10 January may well have drifted through the cold spot (192 K at 26 hPa is the lowest and topmost value; some wave-like temperature variation with height can be seen in Figure 5, sounding (d), but ten values above 100 hPa are far from sufficient for a detailed interpretation).

In summary, a forecasting and analysis system for investigating mesoscale dynamics at stratospheric levels in three dimensions and with good spatial resolution was applied. It had a direct impact on the successful detection of mesoscale polar stratospheric clouds. It is envisaged that experiences gained from detailed hindcasts for all POLECAT and POLSTAR events (which are underway) will help to improve the mountain wave forecasting capabilities for future campaigns.

Acknowledgements

References

Dudhia, J. (1993). A non-hydrostatic version of the Penn State–NCAR Mesoscale Model: validation tests and simulation of an Atlantic cyclone and cold front. *Mon. Wea. Rev.*, **121**: 1493–1513.

Grell, G. A., Dudhia, J. & Stauffer, D. R. (1994). A description of the fifth-generation Penn State/NCAR mesoscale model (MM5). *Technical. Note 398*, National Center for Atmospheric Research, Boulder, USA, 121 pp.

Leutbecher, M. & Volkert, H. (1996). Stratospheric temperature anomalies and mountain waves: a three-dimensional simulation using a multi-scale weather prediction model. *Geophys. Res. Lett.*, **23**: 3329–3332.

Lefevre, F., Brasseur, G. P., Folkins, I., Smith, A. K. & Simon, P. (1994). Chemistry of the 1991–1992 stratospheric winter: three-dimensional model simulations. *J. Geophys. Res.*, **99**: 8183–8195.

Hanson, D. & Mauersberger, K. (1988). Laboratory studies of the nitric acid trihydrate: implications for the south polar stratosphere. *Geophys. Res. Lett.*, **15**: 855–858.

Peter, T., Müller, R., Pawson, S. & Volkert, H. (1995). POLECAT: preparatory and modelling studies. *Phys. Chem. Earth*, **20**: 109–121.

Pyle, J., Carver, G. & Schmidt, U. (1993). ECMWF products in the European Arctic Stratospheric Ozone Experiment (EASOE). *ECMWF Seminar Proceedings 1992*, Vol. II, European Centre for Medium-Range Weather Forecasts, Reading, UK, 1–28.

Schrodin, R. (ed.) (1996). *Quarterly report of the operational NWP-models of the Deutscher Wetterdienst*, No. 8, Deutscher Wetterdienst, Offenbach, 60 pp.

Shutts, G. J., Kitchen, M. & Hoare, P. H. (1988). A large amplitude gravity wave in the stratosphere detected by radiosonde. *Q. J. R. Meteorol. Soc.*, **114**: 579–594.

Volkert, H. & Intes, D. (1992). Orographically forced stratospheric waves over northern Scandinavia. *Geophys. Res. Lett.*, **19**: 1205–1208.

Wirth, M. & Renger, W. (1996). Evidence of large scale ozone depletion within the arctic polar vortex 94/95 based on airborne LIDAR measurements. *Geophys. Res. Lett.*, **23**: 813–816.